

# Evolution of the Proximal Sealing Rings of the Anaconda Stent-Graft After Endovascular Aneurysm Repair

Journal of Endovascular Therapy  
 2018, Vol. 25(4) 480–491  
 © The Author(s) 2018



Reprints and permissions:  
[sagepub.com/journalsPermissions.nav](http://sagepub.com/journalsPermissions.nav)  
 DOI: 10.1177/1526602818773085  
[www.jevt.org](http://www.jevt.org)



Maaïke A. Koenrades, MSc<sup>1,2</sup> , Almar Klein, PhD<sup>2</sup>, Anne M. Leferink, PhD<sup>2</sup> , Cornelis H. Slump, PhD<sup>2</sup>, and Robert H. Geelkerken, MD, PhD<sup>1,2</sup>

## Abstract

**Purpose:** To provide insight into the evolution of the saddle-shaped proximal sealing rings of the Anaconda stent-graft after endovascular aneurysm repair (EVAR). **Methods:** Eighteen abdominal aortic aneurysm patients were consecutively enrolled in a single-center, prospective, observational cohort study (LSPEAS; *Trialregister.nl* identifier NTR4276). The patients were treated electively using an Anaconda stent-graft with a mean 31% oversizing (range 17–47). According to protocol, participants were to be followed for 2 years, during which 5 noncontrast electrocardiogram-gated computed tomography scans would be conducted. Three patients were eliminated within 30 days (1 withdrew, 1 died, and a third was converted before stent-graft deployment), leaving 15 patients (mean age 72.8±3.7 years; 14 men) for this analysis. Evolution in size and shape (symmetry) of both proximal infrarenal sealing rings were assessed from discharge to 24 months using dedicated postprocessing algorithms. **Results:** At 24 months, the mean diameters of the first and second ring stents had increased significantly (first ring: 2.2±1.0 mm,  $p<0.001$ ; second ring: 2.7±1.1 mm,  $p<0.001$ ). At 6 months, the first and second rings had expanded to a mean 96.6±2.1% and 94.8±2.7%, respectively, of their nominal diameter, after which the rings expanded slowly; ring diameters stabilized to near nominal size (first ring, 98.3±1.1%; second ring, 97.2±1.4%) at 24 months irrespective of initial oversizing. No type I or III endoleaks or aneurysm-, device-, or procedure-related adverse events were noted in follow-up. The difference in the diametric distances between the peaks and valleys of the saddle-shaped rings was marked at discharge but became smaller after 24 months for both rings (first ring: median 2.0 vs 1.2 mm,  $p=0.191$ ; second ring: median 2.8 vs 0.8 mm;  $p=0.013$ ). **Conclusion:** Irrespective of initial oversizing, the Anaconda proximal sealing rings radially expanded to near nominal size within 6 months after EVAR. Initial oval-shaped rings conformed symmetrically and became nearly circular through 24 months. These findings should be taken into account in planning and follow-up.

## Keywords

abdominal aortic aneurysm, endograft deployment, endovascular aneurysm repair, expansion, fixation, nitinol ring stent, proximal sealing, ring symmetry, stent-graft

## Introduction

In the past 20 years, the midterm results of endovascular aneurysm repair (EVAR) of abdominal aortic aneurysms (AAAs) have improved, resulting in broader application of this treatment and the commercialization of a multitude of stent-graft designs.<sup>1</sup> The long-term outcome of EVAR, though, still remains a concern,<sup>2</sup> especially since treatment indications are expanding to include not only unfavorable AAA anatomies<sup>3</sup> but also younger, low-risk patients with a long life expectancy.<sup>4</sup>

Durable proximal attachment and sealing are crucial for long-term integrity and depend on the interaction between the proximal stent-graft and the nonaneurysmal infrarenal

or suprarenal aortic wall. A loss of contact with the wall can lead to endoleak and migration, which are the main reasons for reinterventions.<sup>5</sup> Self-expanding stent-grafts rely on a sufficient degree of oversizing to exert a continued outward pressure on the aortic wall in order to provide an adequate

<sup>1</sup>Department of Vascular Surgery, Medisch Spectrum Twente, Enschede, the Netherlands

<sup>2</sup>MIRA Institute for Biomedical Engineering and Technical Medicine, University of Twente, Enschede, the Netherlands

### Corresponding Author:

Maaïke A. Koenrades, Department of Vascular Surgery, Medisch Spectrum Twente, PO Box 50000, 7500 KA Enschede, the Netherlands.  
 Email: [m.a.koenrades@utwente.nl](mailto:m.a.koenrades@utwente.nl)

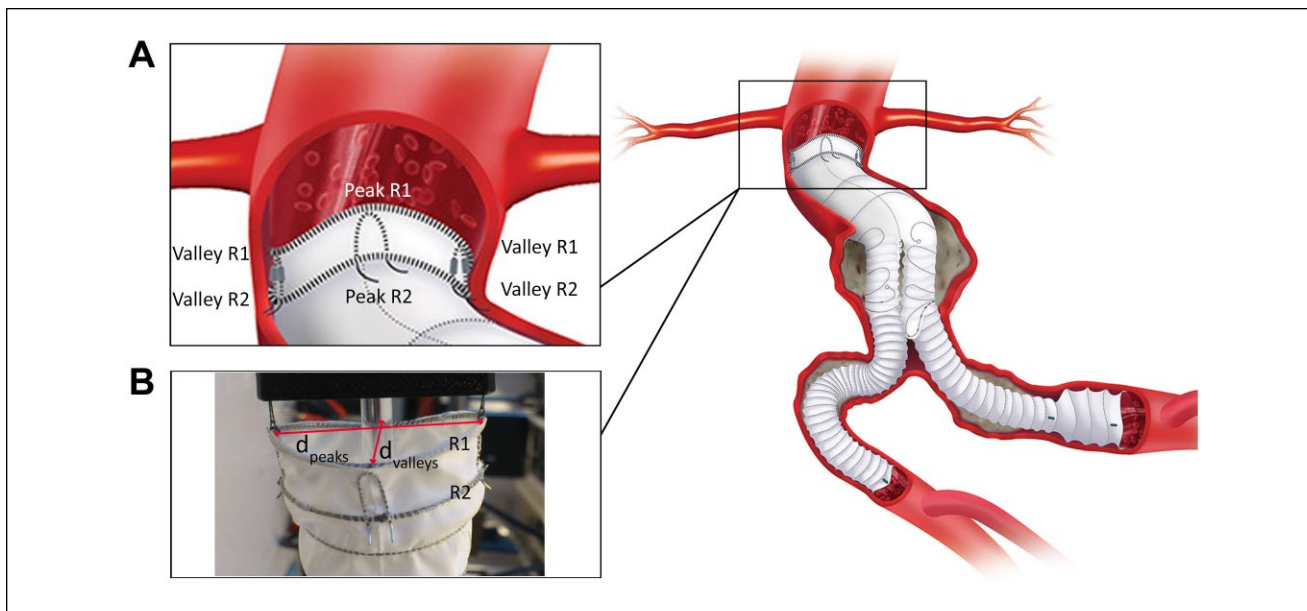


**Figure 1.** A representation (right image) of a deployed Anaconda stent-graft system for the treatment of infrarenal abdominal aortic aneurysm. (A) The proximal part of the main body showing the dual ring in a saddle configuration forming peaks and valleys. (B) Diametric distances analyzed in this study are labeled in the photograph for the first ring stent. R1, first ring stent; R2, second ring stent;  $d_{\text{peaks}}$ , distance between peaks;  $d_{\text{valleys}}$ , distance between valleys. (Schematic illustration was adapted with permission from Vascutek Ltd.)

seal. Self-expanding stent-grafts may conform to the vessel should the aortic neck dilate, which is in contrast to balloon-expandable and sac anchoring devices that do not have such spring-like behavior.

Additionally, there are considerable differences in the sealing and fixation mechanisms among self-expanding stent-graft designs,<sup>1</sup> including but not limited to suprarenal or infrarenal fixation, radial strength, structure of the wire frame, and number of hooks and barbs. Understanding the specific characteristics of each device is paramount in selecting the most appropriate device, size, and deployment technique for each individual patient anatomy and for appreciating potentially harmful adaptations of the aortic neck over time. In addition, such insight can encourage device manufacturers to improve devices to maximize durability.

The Anaconda AAA stent-graft (Vascutek, a Terumo company, Inchinnan, Scotland) is a self-expanding infrarenally fixating device with a proximal dual ring design that assumes a saddle shape with peaks and valleys when oversized and deployed in the aortic neck (Figure 1). The initial design of Lauterjung in 1996 has evolved to a device with favorable midterm results,<sup>6–8</sup> even in severely angulated anatomy.<sup>9,10</sup> From clinical observations, it appears that over time the rings expand and the saddle shape flattens.<sup>11,12</sup> However, the evolution of this change, the relation to oversizing, and the extent and symmetry of ring expansion have not been studied in detail. It is not known whether the rings expand uniformly in the directions of the peaks and valleys or whether the shape of the rings changes over time, which

may be important for long-term integrity of the wall and seal.

The objective of the present study was to investigate the evolution of the postdeployment saddle shape of the Anaconda AAA stent-graft by prospectively evaluating changes in size and shape of the proximal sealing and fixation rings after EVAR.

## Methods

### Study Design and Patient Sample

From April 2014 to May 2015, asymptomatic patients >70 years old with an infrarenal AAA anatomically suitable for elective EVAR using an Anaconda AAA stent-graft were prospectively enrolled in a single-center, observational cohort study [Longitudinal study of pulsatility and expansion in aortic stent-grafts (LSPEAS); registered on *Trialregister.nl* identifier NTR4276] designed to investigate factors influencing the success or failure of proximal stent-graft fixation and sealing. The study protocol was approved by the institutional review board. Written informed consent was obtained for each subject before participation in the study.

Patients were screened to evaluate their suitability for elective EVAR and inclusion in the trial. The screening consisted of a general health analysis, including the Society of Vascular Surgery<sup>13</sup> risk scores, as well as the American Society of Anesthesiologists classification.<sup>14</sup> Spiral computed tomography angiography (CTA) was performed

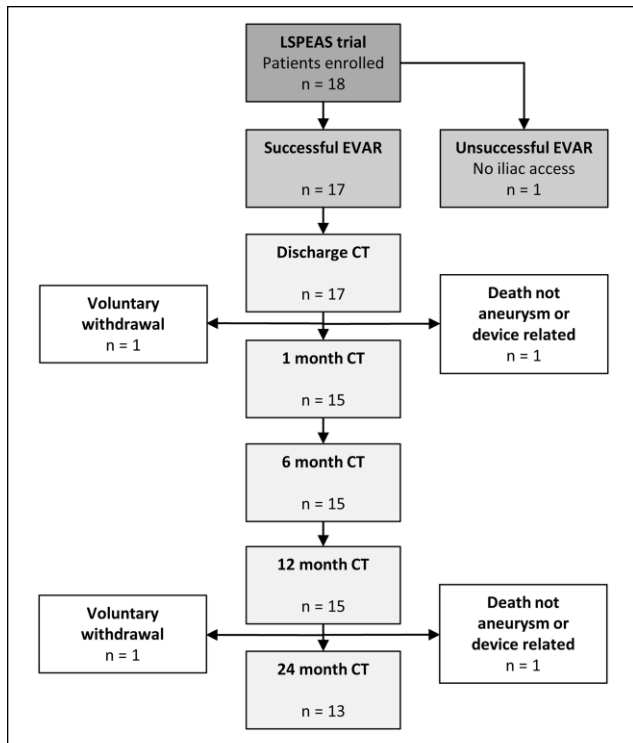


**Figure 2.** Chart showing the flow of patients enrolled in the LSPEAS (Longitudinal study of pulsatility and expansion in aortic stent-grafts) trial. CT, computed tomography; EVAR, endovascular aneurysm repair.

according to standard practice to define aneurysm anatomy according to the EUROSTAR criteria.<sup>15,16</sup> By protocol, non-contrast electrocardiogram (ECG)-gated CT scans were performed before intervention, before discharge, and after 1, 6, 12, and 24 months of follow-up. In addition, after 1 month, participants underwent duplex ultrasound at the subsequent visits to evaluate the presence of endoleaks. Only patients who were able to comply with these requirements were eligible for the study.

Of the 18 patients enrolled in the LSPEAS trial during the observation period, 1 patient withdrew within 30 days, 1 patient died within 30 days (pulmonary embolism), and a third patient was converted to open repair owing to iliac access issues, leaving 15 patients (mean age 72.8±3.7 years; 14 men) who completed the minimum 12-month follow-up (Figure 2). Patient characteristics and aneurysm characteristics of the 15 patients are summarized in Table 1.

Patient demographic data and information on implanted stent-graft diameters were obtained from the patient registry. Stent-grafts were sized from inner wall diameters. Oversizing was increased in case of unfavorable neck anatomy, including reversed conical and short necks, and for inclined placement (ie, nonperpendicular to the flow axis) in angulated necks, resulting in a broad range of initial oversizing (mean 31%, range 17–47%).

**Table 1.** Patient and Aneurysm Characteristics.<sup>a</sup>

Demographics/risk factors	
Age, y	72.8 (70–80)
Men	14
Body mass index, kg/m <sup>2</sup>	26.8 (22.2–34.7)
ASA grade I / II / III	2 / 12 / 1
Smoking	7
Hypertension	14
Hyperlipidemia	12
Cardiac disease	7
Stroke / TIA	1 / 2
Renal disease	1
Pulmonary disease	2
Aneurysm	
EUROSTAR <sup>b</sup> A / B / C / D / E	1 / 8 / 1 / 4 / 1
Infrarenal neck diameters, mm	22 (18–28)
D2a	22 (18–28)
D2b	23 (19–29)
D2c	23 (19–29)
Neck shape <sup>c</sup> I / II / III / IV	9 / 4 / 1 / 1
Neck length, mm	35 (20–75)
Circumferential calcification	
D2a / b / c, %	50 / 60 / 80
D2a / b / c >25%	2
Luminal thrombus	
D2a / b / c, %	0 / 30 / 35
D2a / b / c >25%	1
Infrarenal neck angulation, deg >60°	43 (0–110) <sup>d</sup>
	4
Maximum AAA diameter	60 (40–70) <sup>e</sup>
Main device diameters, mm	
25.5 (OLB 25)	1
28 (OLB 28)	5
30.5 (OLB 30)	6
32 (OLB 32)	1
34 (OLB 34)	2
Oversizing, <sup>f</sup> %	31 (17–47)

Abbreviations: AAA, abdominal aortic aneurysm; ASA, American Society of Anesthesiologists; OLB, main body device size; TIA, transient ischemic attack.

<sup>a</sup>Continuous data are presented as the means (range); categorical data are given as the counts.

<sup>b</sup>EUROSTAR AAA morphology.<sup>15</sup>

<sup>c</sup>Neck shape according to Balm et al.<sup>14</sup>

<sup>d</sup>Two patients with angulation >90° were positioned with 90° rotation (saddle peaks in lateral direction and valleys and legs in anteroposterior direction).

<sup>e</sup>One AAA <50 mm but with 38-mm iliac aneurysms (EUROSTAR category D).

<sup>f</sup>Device size was based on inner wall diameters.

### Device Description

The Anaconda AAA stent-graft system and implantation procedure have been extensively described elsewhere.<sup>6,8,17</sup> In short, the Anaconda stent-graft is a repositionable 3-piece endovascular graft for infrarenal fixation and consists of a woven polyester graft supported by independent nitinol ring

stents that each comprise a single strand of wound nitinol wire, that is, a wire bundle (Figure 1). The proximal part of the main body consists of a self-expanding dual ring, which assumes the shape of a “saddle” when oversized and constrained against the aortic wall. When unconstrained, the shape of the rings is circular. The first ring stent (R1) has a larger wire bundle diameter (higher number of wire turns) compared to the second ring stent (R2), resulting in a higher radial strength compared to R2. The larger the main body size, the larger the wire bundle diameter (R1, 0.7–1.0 mm; R2, 0.5–0.7 mm).

The peaks of the saddle (convexities) are commonly placed in an anteroposterior direction with the valleys (concavities) placed in a lateral direction, but a 90° rotated placement may also be applied in case of severe neck angulation. The peaks are placed just below or at the level of the renal arteries. Active fixation is provided by 4 pairs of hooks, which are attached to both proximal rings at the peaks and valleys. The body is available in diameters ranging from 21.5 to 34 mm for aortic vessel inner diameters of 17.5 to 31 mm. The instructions for use (IFU) advise a neck length  $\geq 15$  mm, infrarenal angulation  $\leq 90^\circ$ , and an oversizing range from 10% to 20% with regard to inner vessel wall diameter.<sup>18</sup>

### Image Acquisition

ECG-gated CT scans were performed on an Aquilion 64 CT scanner (Toshiba Medical Systems Corporation, Tokyo, Japan) or on a Somatom Definition Flash CT scanner (Siemens Healthcare, Erlangen, Germany) with a standardized low-dose scan protocol based on the routine static protocol for the abdomen. The 24-month scans were exclusively acquired on the Somatom Flash scanner. The scans were performed without contrast administration to preclude nephrotoxic effects. Scan parameters were as follows: rotation time 0.4 seconds (Aquilion), 0.3 seconds (Flash); collimation 64×0.5 mm (Aquilion), 2×128×0.6 mm (Flash); slice thickness 1 mm; slice increment 0.5 mm; reconstructed matrix size 512×512 pixels, resulting in submillimeter isotropic datasets. The pitch factor was set automatically based on the heart rate. Tube voltage was set to 120 kV with a tube current time product of 40, 60, or 80 mA·s based on the patient's body mass index (<20, 20–25, >25 kg/m<sup>2</sup>, respectively), since automated tube current modulation had to be turned off for ECG tracking. This resulted in a dose length product of 962.1±220.1 mGy·cm for a scan length of ~30 cm. Images were acquired during a single breath hold after performing a standard breathing exercise. Retrospective gating was applied to obtain 10 equidistant volumes covering the cardiac cycle.

### Image Processing

The image processing steps included obtaining a phase-averaged 3-dimensional (3D) volume and segmentation of

the 2 proximal sealing rings of the Anaconda stent-graft. Because a low-dose protocol for ECG-gated CT data was used, the exposure dose per reconstructed phase was decreased in comparison to a static CT scan, resulting in lower signal-to-noise (SNR) reconstructions. Since averaging the individual phases would result in a 3D volume that was subject to motion artifacts, a nonrigid B-spline registration was applied to obtain motion-compensated, time-averaged 3D volumes with improved SNR. A previously described registration algorithm<sup>19,20</sup> that was adjusted and validated for the purpose of stent-graft analysis in ECG-gated CT data<sup>21</sup> was used.

The time-averaged 3D volumes, which represented mid cardiac cycle, were used for segmentation of the dual ring and evaluation of the aortic vessel. Geometric models of the dual ring were obtained by applying a segmentation algorithm that was designed for stent analysis in volumetric CT data.<sup>22</sup> This 3-step segmentation algorithm used a minimum cost path (MCP) method to create a graph consisting of nodes and edges, where the edges represent the wire frame and the nodes are placed on the edges at wire crossings. In short, seed points that are likely to be on the wire frame of the stent-graft are detected (step 1), after which the MCP algorithm connects these seed points by tracing low-cost paths (step 2), that is, short paths between seed points through high-intensity voxels, resulting in a graph consisting of nodes that are connected by edges. Finally, because many of the traced edges do not fully run on the wire frame, an iterative cleaning operation (step 3) was performed to remove false edges and preserve only those that run through the middle of the wire bundle.

The algorithm was adjusted to allow for manual placement of additional seeds in order to prevent errors in the graph at the level of 2 high-intensity radiopaque markers on the hook struts. Further, a modification was made to allow for interactive restoration of edges in the graph that were falsely removed by the algorithm. False removal occurred in some cases with prominent intensity differences in the CT data between the first ring, the second ring, and the hooks. Finally, 1D quadratic polynomial fits in the  $x$ ,  $y$ , and  $z$  directions were implemented to obtain subvoxel positions. All segmentations were visually inspected in 3D maximum intensity projections.

### Analysis

The evolution over time of the size and shape of the proximal sealing rings was evaluated by measuring the diametric distances between the peaks ( $d_{\text{peaks}}$ ) and the valleys ( $d_{\text{valleys}}$ ) of the saddle-shaped rings in the segmented models through 24 months (Figure 1). The positions of the peaks and valleys on R1 and R2 were obtained as the midpoints between the nodes at each of the 4 hook pair crossings with R1 and R2. Ring diameter was calculated as the mean of  $d_{\text{peaks}}$  and

$d_{\text{valleys}}$  (Equation 1). In addition to ring diameter, the degree of ring expansion was calculated as a percentage of the ring diameter divided by the predetermined flat ring diameter, that is, the nominal diameter as provided by the manufacturer (Equation 2). To evaluate changes in the shape of the rings, an asymmetry ratio was calculated as the maximum to minimum diametric distances between the peaks and valleys (Equation 3). For the purpose of visualizing the direction of asymmetry, the asymmetry ratio was also calculated by dividing  $d_{\text{peaks}}$  by  $d_{\text{valleys}}$ . Additionally, the difference between the diametric distances was evaluated during follow-up.

$$\text{Ring diameter} = \frac{d_{\text{peaks}} + d_{\text{valleys}}}{2} \quad (1)$$

$$\text{Ring expansion percentage} = \frac{\text{ring diameter}}{\text{nominal ring diameter}} \times 100 \quad (2)$$

$$\text{Asymmetry ratio} = \frac{\max(d_{\text{peaks}}, d_{\text{valleys}})}{\min(d_{\text{peaks}}, d_{\text{valleys}})} \quad (3)$$

### Statistical Analysis

Normality checks were performed to assess the distribution of the data, which are presented as means  $\pm$  standard deviation (range) for normally distributed continuous variables and as numbers for categorical variables. The median (interquartile range, IQR) is also given for non-parametric data.

Parametric data were compared between time points by use of a one-way analysis of variance (ANOVA) for repeated measures. For nonparametric data, the Friedman test was used instead with post hoc analysis using the Wilcoxon signed-rank test. The difference between diametric peak and valley distances was also compared at each time point for all patients in follow-up by using the Student *t* test for paired data. Test results are presented with the 95% confidence interval (CI). Statistical significance was assumed when  $p < 0.05$ . A Bonferroni-adjusted significance level of  $p < 0.01$  was used for nonparametric data. Statistical analysis was performed using SPSS Statistics (version 24.0; IBM Corporation, Armonk, NY, USA).

### Results

No aneurysm-, device-, or procedure-related adverse events were reported through the 24-month follow-up in 13 of the 15 patients [1 patient died (carcinoma) and 1 patient withdrew]. The mean aneurysm sac diameter decreased from  $60 \pm 7$  mm at discharge to  $44 \pm 12$  mm after 24 months, with at least 5-mm sac diameter regression in 10 patients.

### Evolution of the Proximal Rings

Figure 3 presents the change in size of the dual rings from discharge to 24 months, as both the ring stent diameters and a percentage of their nominal size, that is, postdeployment ring expansion. For all patients, the diameter of both ring stents increased over time. From discharge to 24 months after EVAR, the mean ring diameter increased significantly by  $2.2 \pm 1.0$  mm (95% CI 1.2 to 3.2,  $p < 0.001$ ) for R1 and  $2.7 \pm 1.1$  mm (95% CI 1.7 to 3.8,  $p < 0.001$ ) for R2 (Table 2). The maximum increase in ring diameter at 24 months was 5.0 mm (23%); however, the maximum increase in diametric distance ( $d_{\text{peaks}}$  or  $d_{\text{valleys}}$ ) was 7.7 mm (34%) for a patient with an initial asymmetry ratio of 1.5. The mean ring diameter increased most between discharge and 1 month for both rings, with a mean difference of  $1.1 \pm 0.8$  mm (95% CI 0.3 to 1.8,  $p = 0.003$ ) for R1 and  $1.1 \pm 0.8$  mm (95% CI 0.3 to 1.8,  $p = 0.004$ ) for R2. Through 24 months, the mean percentage of ring expansion increased significantly by  $7.6\% \pm 3.8\%$  (95% CI 4.0% to 11.2%,  $p < 0.001$ ) for R1 and by  $9.4\% \pm 4.1\%$  (95% CI 5.5% to 13.3%,  $p < 0.001$ ) for R2. The percentage increase was greatest during the first month for both ring stents ( $p = 0.005$ ) and highest in the 3 patients with the most pronounced saddle shapes because of greater oversizing (33%, 40%, and 47%). At 6 months, the rings had significantly expanded to a mean level of  $96.6\% \pm 2.1\%$  for R1 and  $94.8\% \pm 2.7\%$  for R2. After 6 months, the expansion percentage increased slowly, and the ring diameters stabilized close to their nominal size irrespective of the initial oversizing ( $98.3\% \pm 1.1\%$  for R1 and  $97.2\% \pm 1.4\%$  for R2 at 24 months).

Figure 4 presents the evolution of ring shape for each individual patient, showing the asymmetry ratio of  $d_{\text{peaks}}$  to  $d_{\text{valleys}}$ . At discharge, this ratio had a broad range of 0.65 to 1.21 for R1 and 0.72 to 1.50 for R2, but at 24 months, this range had narrowed to 0.94 to 1.11 for R1 and 0.94 to 1.24 for R2, meaning that the oval-shaped rings had adapted to be more circular. For R1, the average asymmetry ratio did not significantly change from discharge to 24 months ( $p = 0.079$ ), but a significant difference was found for R2 ( $p = 0.009$ ; Table 2). The difference between the diametric peak and valleys distances was significant ( $p < 0.005$ ) at all time points for both rings, yet compared with discharge this difference had become smaller after 24 months (R1: median 2.0 vs 1.2 mm,  $p = 0.191$ ; R2: median 2.8 vs 0.8 mm,  $p = 0.013$ ).

In Figure 5, the evolution of ring stent shape through 24 months is visualized for a patient with a pronounced saddle-shaped dual ring at discharge, showing the adaptation from an asymmetric saddle to flattened symmetric ring stents. Note that in this case the orientation of ring stent asymmetry changed during the first month. In this patient, the diameter of the aneurysm sac decreased from 65 mm at discharge to 37 mm after 24 months.

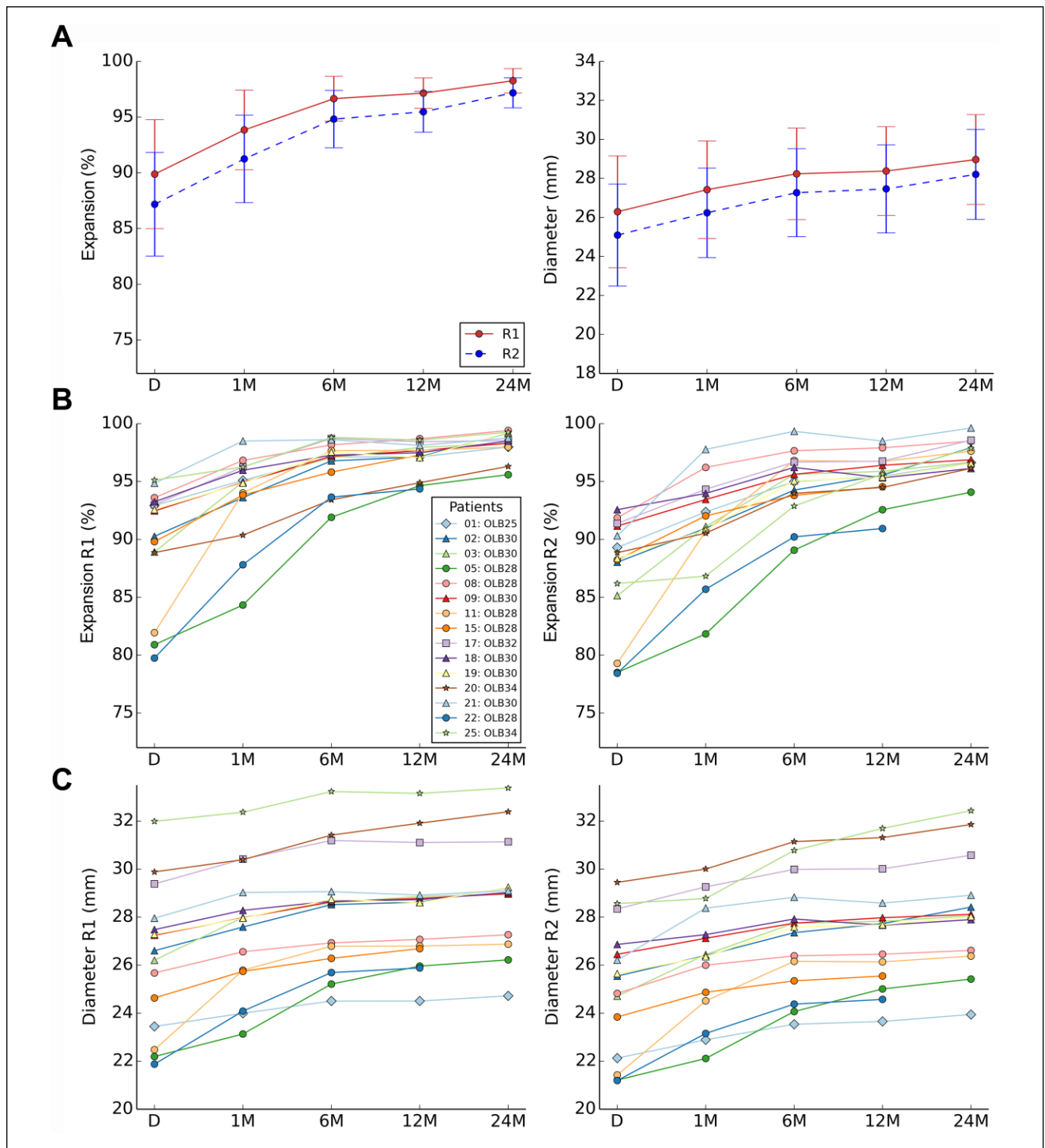


**Figure 3.** Evolution of the proximal dual ring of the Anaconda stent-graft from discharge to 24 months after endovascular aneurysm repair (EVAR), presented as the mean (dot) and standard deviation (whiskers) of the (A) expansion percentage (diameter ring / nominal diameter ring × 100) and the ring diameter  $[(d_{peaks} + d_{valleys}) / 2]$  for both rings and (B, C) for each individual patient for both rings. D, discharge; M, months after EVAR; OLB, main body device size; R1, first ring stent; R2, second ring stent.

**Discussion**

In this study, substantial variation in the initial size of the dual rings was observed per patient and per ring stent,

though the first ring had consistently expanded further compared to the second ring. Interestingly, despite this initial variation, there was consistent expansion of the saddle-shaped rings to near nominal size irrespective of the initial

**Table 2.** Evolution of the Size and Shape of the Proximal Sealing Rings Through the 24-Month Follow-up.<sup>a</sup>

	Discharge (n=15)	1 Month (n=15)	6 Months (n=15)	12 Months (n=15)	24 Months (n=13)
Expansion R1, <sup>b</sup> %	89.9±5.1 (79.7–95.1)	93.8±3.7 (84.3–98.5)	96.6±2.1 (91.9–98.8)	97.1±1.4 (94.4–98.7)	98.3±1.1 (95.6–99.4)
	—	p=0.005	p<0.001	p<0.001	p<0.001
Expansion R2, <sup>b</sup> %	87.2±4.8 (78.4–92.6)	91.2±4.1 (81.8–97.8)	94.8±2.7 (89.1–99.3)	95.5±1.9 (90.9–98.5)	97.2±1.4 (94.1–99.6)
	—	p=0.005	p<0.001	p<0.001	p<0.001
Diameter change R1, <sup>c</sup> mm	—	1.1±0.8 (0.4–3.3)	1.9±1.0 (1.1–4.3)	2.1±1.1 (1.0–4.3)	2.2±1.0 (1.2–4.4)
	—	p=0.003	p<0.001	p<0.001	p<0.001
Diameter change R2, <sup>c</sup> mm	—	1.1±0.8 (0.2–3.1)	2.2±1.0 (1.1–4.7)	2.4±1.1 (0.8–4.7)	2.7±1.1 (1.0–5.0)
	—	p=0.004	p<0.001	p<0.001	p<0.001
Asymmetry ratio R1 <sup>d</sup>	1.12±0.14 (1.02–1.55)	1.10±0.11 (1.01–1.40)	1.09±0.07 (1.01–1.31)	1.07±0.07 (1.00–1.27)	1.05±0.03 (1.00–1.11)
	1.07 [1.03, 1.16]	1.07 [1.01, 1.15]	1.08 [1.04, 1.09]	1.06 [1.03, 1.09]	1.04 [1.03, 1.08]
	—	p=0.430	p=0.236	p=0.058	p=0.079
Asymmetry ratio R2 <sup>d</sup>	1.17±0.16 (1.02–1.50)	1.14±0.14 (1.02–1.48)	1.10±0.09 (1.03–1.31)	1.08±0.07 (1.00–1.24)	1.06±0.07 (1.00–1.24)
	1.12 [1.04, 1.24]	1.09 [1.04, 1.17]	1.07 [1.04, 1.12]	1.06 [1.03, 1.12]	1.03 [1.02, 1.10]
	—	p=0.146	p=0.027	p=0.010	p=0.009
Difference $d_{\text{peaks}} - d_{\text{valleys}}$ R1, mm	2.7±2.7 (0.4–10.2)	2.4±2.5 (0.2–8.3)	2.2±1.7 (0.2–6.9)	1.9±1.6 (0.0–6.1)	1.5±1.0 (0.1–3.2)
	2.0 [0.6, 4.4]	2.1 [0.2, 4.0]	1.9 [1.1, 2.5]	1.6 [0.8, 2.5]	1.2 [0.8, 2.2]
	—	p=0.635	p=0.331	p=0.131	p=0.191
Difference $d_{\text{peaks}} - d_{\text{valleys}}$ R2, mm	3.6±3.3 (0.4–11.2)	3.2±3.0 (0.5–10.8)	2.6±2.1 (0.8–7.3)	2.2±1.8 (0.6–6.8)	1.7±1.7 (0.1–5.8)
	2.8 [1.0, 5.4]	2.4 [0.8, 4.0]	2.0 [1.0, 3.2]	1.5 [0.8, 3.0]	0.8 [0.4, 2.6]
	—	p=0.366	p=0.046	p=0.013	p=0.013

Abbreviations: R1, first ring stent; R2, second ring stent.

<sup>a</sup>Data are presented as the means ± standard deviation (range) and median [interquartile range Q1, Q3] as applicable. P values refer to discharge vs other time points.

<sup>b</sup>Expansion percentage = (diameter / nominal diameter) × 100.

<sup>c</sup>Diameter =  $(d_{\text{peaks}} + d_{\text{valleys}}) / 2$ .

<sup>d</sup>Asymmetry ratio =  $\max(d_{\text{peaks}}, d_{\text{valleys}}) / \min(d_{\text{peaks}}, d_{\text{valleys}})$ .

degree of oversizing (Figure 3). Expansion of the rings occurred mostly within the first 6 months after EVAR, with the greatest degree of expansion during the first month and in patients with the most pronounced saddle shapes (greater oversizing). An explanation for this observation could be found in the stress-strain curve of nitinol; after release of the stent-graft from the delivery system, the force can be initially higher at higher deflection<sup>23</sup> and thus greater oversizing. Notably, in one of these patients the ring stents expanded rapidly within 1 month, while in the other 2 patients the saddle shape was preserved for a longer period of time (Figure 3). The reason for this could be differences in aortic wall characteristics (ie, stiffness), since there were some calcifications at the level of the dual rings in the latter 2 patients.

Another important finding of this work is that during the course of ring expansion the oval-shaped ring stents conform symmetrically and become circular. This process may take >2 years when the initial shape is highly asymmetric (Figure 4). Specifically the 3 patients with the most marked infrarenal neck angulation (>70°) showed the highest degree of ring stent asymmetry (Figure 6). These results imply that over time the aortic neck deforms due to the radial force of the ring stents. Additionally, these adaptations of the aortic neck may have implications for the durability of the seal and fixation. However, clinical midterm data on the Anaconda shows that migration and endoleak rates are low,<sup>6–8</sup> even in severely angulated proximal necks.<sup>9,10</sup>

Recently, the largest published single-center clinical experience using the Anaconda reported a 1.1% rate of late type Ia endoleak and no migration at a mean follow-up of

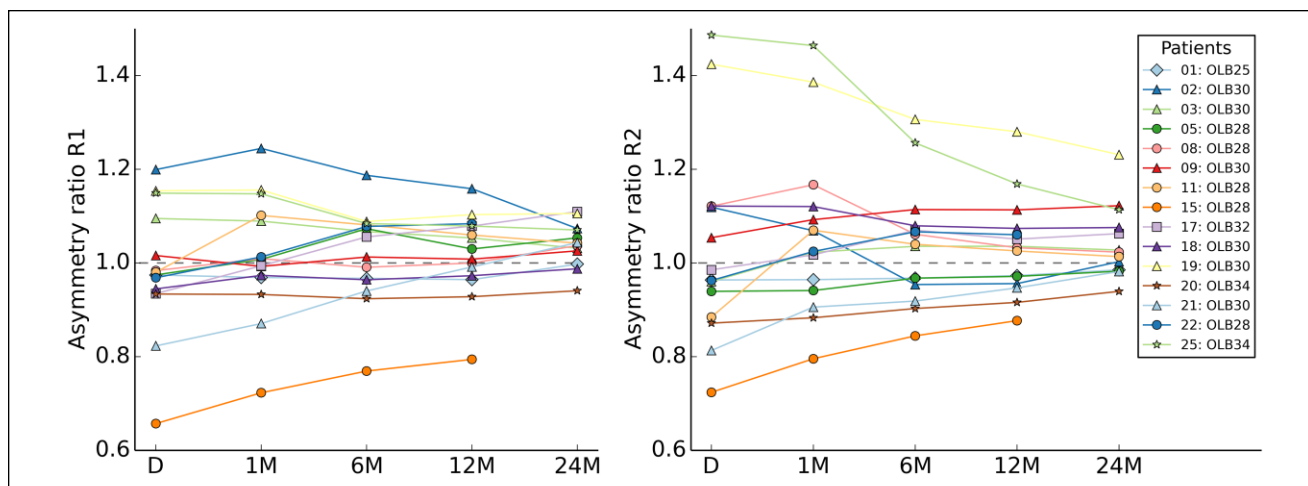


**Figure 4.** Evolution of the asymmetry ratio of the proximal dual ring of the Anaconda stent-graft from discharge to 24 months after endovascular aneurysm repair (EVAR). Here, for the purpose of visualizing the direction of asymmetry, the asymmetry ratio of each ring was calculated as  $d_{\text{peaks}}/d_{\text{valleys}}$  at a given time. The dashed line is a ratio of 1.0, which represents symmetric ring dimensions. In 2 cases (#19 and #25), the body was positioned with 90° rotation (saddle peaks in lateral direction and valleys in anteroposterior direction). D, discharge; M, months after EVAR; OLB, main body device size; R1, first ring stent; R2, second ring stent.

32.9±23.3 months.<sup>7</sup> In our present cohort no clinical failures related to device migration or endoleak were observed, which is reflected in the regression of aneurysm sac diameters in the majority of patients. To our knowledge, no reports have been published on the symmetry of ring expansion in other self-expanding stent-grafts.

Because the ring stents continue to expand to near nominal size, the vessel wall is subjected to tensile stress and may undergo several millimeters of dilatation at the level of the sealing and fixation rings, depending on the degree of oversizing. Also, when asymmetric ring stents become circular, the degree of ring expansion over a single axis can be extensive (>5 mm). These significant levels of ring expansion may raise concerns related to aortic neck dilatation (AND), which has been associated with migration, endoleak, and increased reintervention rates.<sup>24–27</sup> However, ring expansion also enhances apposition between the graft and the vessel wall. Moreover, local dilatation due to ring expansion does not necessarily result in dilatation of the entire neck. In fact, ring expansion at only the sealing zone may prevent the stent-graft from migrating. In that sense, local proximal radial strength might be preferred over designs that have radial stents through the length of the device. Also, expansion of the rings seems to support embedding of the hooks into the vessel wall (Figure 5), which a few millimeters of migration can facilitate.

Nevertheless, it must be acknowledged that if the neck becomes diseased and subject to progressive AND, the dimensions of the neck could exceed the dimensions of the fully expanded stent-graft. In this case, an opening between the wall and the graft and/or migration may occur, resulting in type Ia endoleak. Our results suggest that after 6 months

the ring stents have little remaining expansion capacity to adapt to potential progressive AND, while others have assumed that in case of progressive AND, the ring stents adapt and the saddle flattens.<sup>11,12</sup>

Certainly, all self-expanding stent-grafts have the limitation that they will accommodate vessel dilatation only up to the point where it reaches their designed diameter. Of importance is whether dilatation of the aortic neck continues after the stent-graft has fully expanded. Monahan et al<sup>28</sup> investigated AND after implantation of the Zenith stent-graft and found that the neck dilates until the stent-graft has approximated its designed diameter. They found that the rate of neck expansion was greatest at early follow-up intervals (1–6 months). Moreover, they concluded that this dilatation is not associated with type I endoleak. Interestingly, 2 other studies that investigated self-expanding stent-grafts reported that AND occurred specifically within the first 6 months but then stabilized through 24 months.<sup>29,30</sup> Also Cao et al<sup>24</sup> concluded that AND is common at midterm follow-up but shows little tendency to progress at a mean follow-up of 18 months, although late reintervention was most frequently necessary in a small number of patients who developed severe ongoing AND. Although several studies do raise concern regarding continuing AND,<sup>4,31</sup> these results imply that midterm AND is not necessarily a clinical problem and may be misinterpreted from the observation of stent-graft expansion. Moreover, the apparent absence of AND after treatment with balloon-expandable stent-grafts,<sup>32,33</sup> which do not exert continued radial force, supports this hypothesis.

The design of the Anaconda allows that the peaks of the proximal saddle-shaped ring can be placed at the level of or just above the renal artery origins, without actually



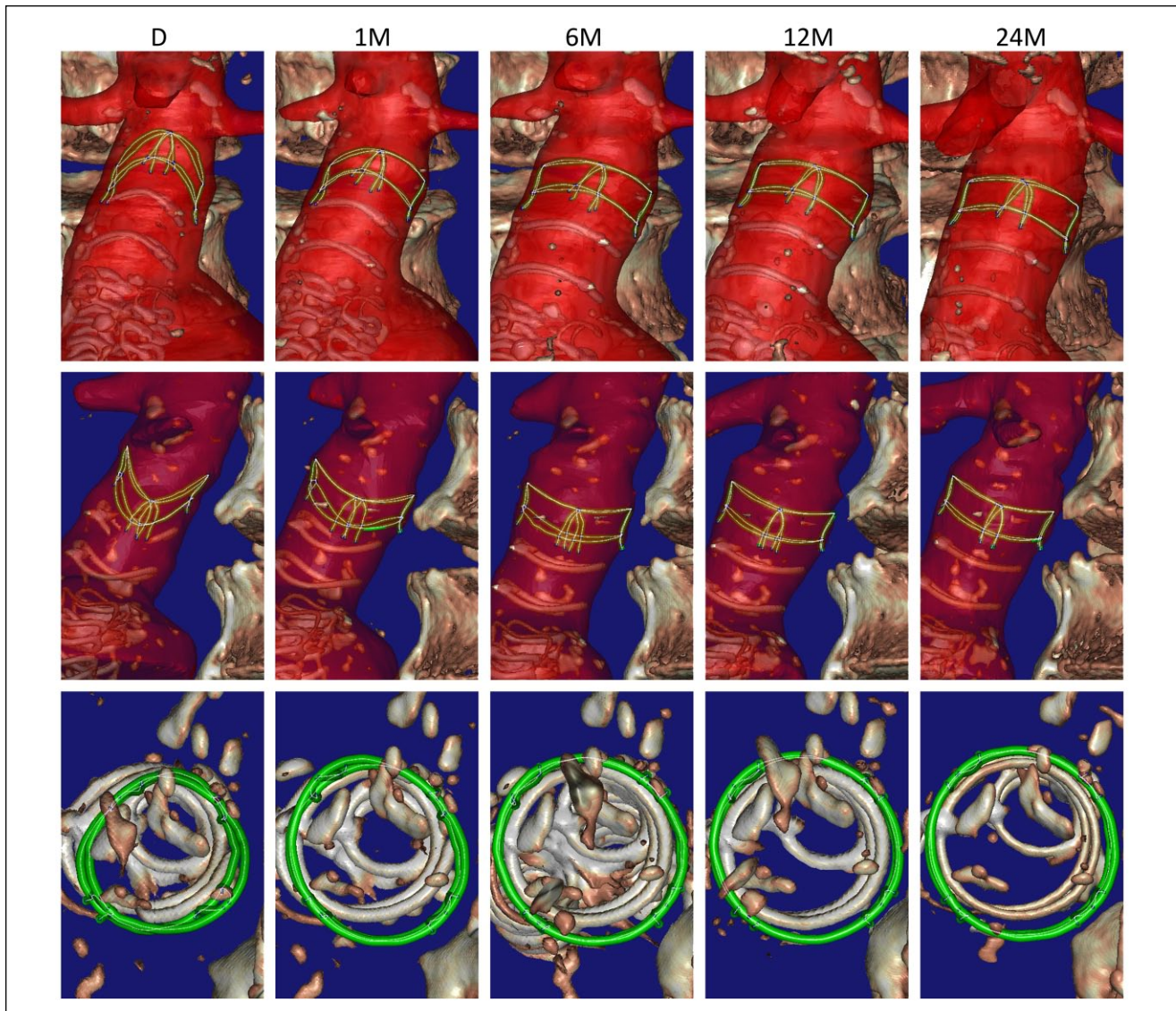


**Figure 5.** A clinical case (#11) demonstrating the evolving adaptation of the proximal sealing and fixation rings from discharge to 24 months after endovascular aneurysm repair (EVAR). The illustration shows anterior to posterior views (top), lateral views from left to right (middle), and top views from superior to inferior (bottom) with the model rotated to be perpendicular to the screen. The model obtained by segmentation is shown in green, with the white lines and blue dots representing the edges and nodes in the model, respectively. The vertebrae, remaining part of the stent-graft, and calcifications are visualized as a surface rendering. A segmentation of the aortic vessel (outer wall), including the proximal part of the renal arteries and superior mesenteric artery, is shown in red. D, discharge; M, months after EVAR.

covering these ostia with the valley of the ring. However, when the proximal rings expand, becoming more circular and the saddle shape flattens, the valleys of the proximal ring may come up a few millimeters, with the potential risk of covering the renal artery ostia.<sup>6,7</sup> Although renal artery occlusion due to upstream migration of the valleys seems to be rare, the clinical consequences can be substantial.<sup>8,9</sup> Whether the valleys indeed migrate upstream or whether the complete proximal device migrates further downstream is the subject of current investigation.

Finally, the evolution of ring stent expansion may differ per design. Also, the behavior of suprarenal fixing devices could differ from what has been observed in the present study, since the stiffness and thickness of the suprarenal and infrarenal vessel segments are different.<sup>34</sup> Therefore, future work should also study the behavior of suprarenally fixing devices, including fenestrated EVAR, especially since there is growing evidence that suprarenal fixation results in a slightly higher risk of renal complications.<sup>35</sup>

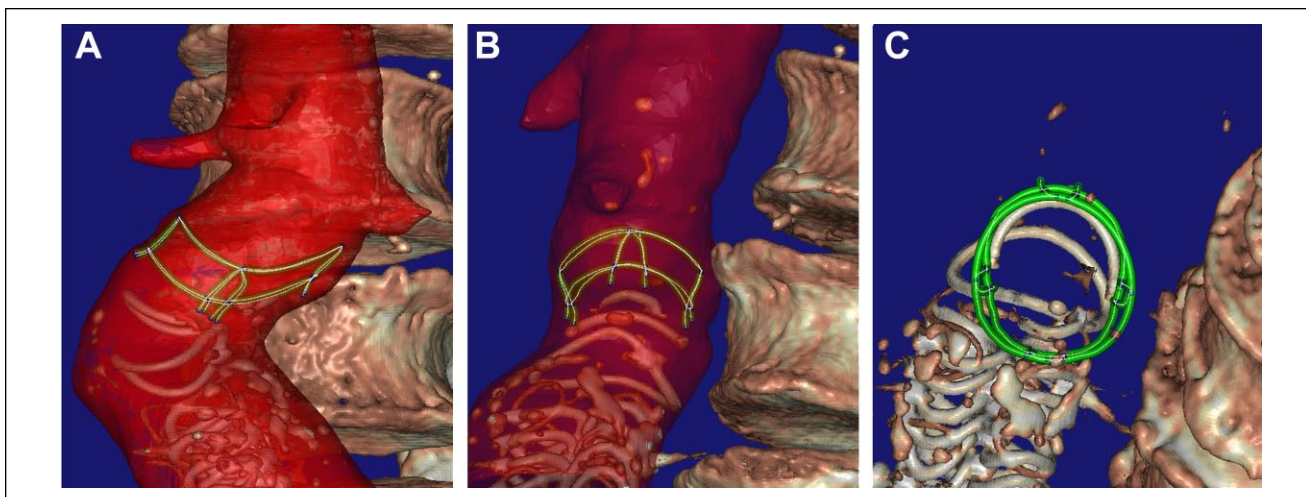


**Figure 6.** A clinical case (#19) with a high degree ( $>90^\circ$ ) of infrarenal neck angulation (outside the instructions for use) demonstrating asymmetric ring dimensions at discharge in the (A) anteroposterior view, (B) lateral view, and (C) oblique craniocaudal view with the model of the dual ring perpendicular to the screen. The main body was positioned with  $90^\circ$  rotation to allow the proximal rings and the anteroposteriorly positioned legs to better follow the course of the angulation. Both rings were not positioned in line with the aorta but rather inclined.

In sum, it is of utmost importance to understand the sealing and fixation behavior of individual stent-graft designs to be able to recognize adaptations of the aortic neck that occur due to the fixation mechanism of the stent-graft itself, rather than disease progression, which may not have further clinical consequences. Additionally, knowledge of stent-graft–neck interactions for both infra- and suprarenal fixating stent-grafts is crucial for selection of the best device, size, and deployment technique based on each patient's aneurysm anatomy.

### Limitations

A potential shortcoming of this study is the low number of patients. Nevertheless, because of the prospective design of the LSPEAS trial, follow-up examinations at 5 standardized time points through 24 months could be obtained. Even though the present number of patients is not enough to evaluate clinical outcome, it does allow for a detailed evaluation of stent-graft behavior. In addition, the results demonstrated clear trends and significant changes. Also, ECG-gated CT scans and advanced postprocessing using an algorithm specifically designed to analyze stents in volumetric CT data allowed accurate repeated measurements at the same time during the cardiac cycle, which is not possible with static CT scans.

### Conclusion

This prospective study has provided insight into the evolution of the proximal sealing and fixation rings of the Anaconda AAA stent-graft system. The saddle-shaped rings

radially expanded to near nominal size within 6 months after EVAR despite a broad range of initial oversizing, all without type I or III endoleak. Interestingly, the asymmetrically shaped ring stents conformed symmetrically and became nearly circular through 24 months. These observations imply that over time the aortic neck conforms to the size of the self-expanding nitinol rings irrespective of neck characteristics. It is therefore advisable to avoid excessive oversizing. Furthermore, one should be careful not to misinterpret neck dilatation due to ring expansion for disease progression while at the same time being alert if the neck continues to dilate after 6 to 12 months when the rings have expanded to their designed size. Local dilatation of the neck due to ring expansion is beneficial for the fixation and sealing as long as neck dilatation is localized exclusively to the sealing zone. Additional research is necessary to investigate potential dilatation of the entire neck and the relation with postoperative ring expansion.

### Acknowledgments

The authors are grateful to Anja Stam (clinical research officer, Department of Surgery, Medisch Spectrum Twente) for her assistance in conducting the LSPEAS trial and to Bert Klein Rot (chief laboratory technician CT, Department of Radiology, Medisch Spectrum Twente) for his technical support with the CT acquisitions. Furthermore, the authors thank all vascular surgeons for including patients in the LSPEAS trial.



### Declaration of Conflicting Interests

The author(s) declared the following potential conflicts of interest with respect to the research, authorship, and/or publication of this article: Robert H. Geelkerken is a consultant for Vascutek Ltd.

## Funding

The author(s) disclosed receipt of the following financial support for the research, authorship, and/or publication of this article: The LSPEAS trial (*Trialregister.nl*; identifier NTR4276) was supported in part by an unrestricted research grant from Vascutek Ltd, a TERUMO Company, and in part by the Dutch Ministry of Economic Affairs under TKI-Allowance under the TKI-programme Life Sciences & Health.

## ORCID iDs

Maaïke A. Koenrades  <https://orcid.org/0000-0003-4555-0551>  
Anne M. Leferink  <https://orcid.org/0000-0002-3765-8450>

## References

- Smeds MR, Charlton-Ouw KM. Infra-renal endovascular aneurysm repair: New developments and decision making in 2016. *Semin Vasc Surg.* 2016;29:27–34.
- Arko FR 3rd, Murphy EH, Boyes C, et al. Current status of endovascular aneurysm repair: 20 years of learning. *Semin Vasc Surg.* 2012;25:131–135.
- Antoniou GA, Georgiadis GS, Antoniou SA, et al. A meta-analysis of outcomes of endovascular abdominal aortic aneurysm repair in patients with hostile and friendly neck anatomy. *J Vasc Surg.* 2013;57:527–538.
- Diehm N, Dick F, Katzen BT, et al. Aortic neck dilatation after endovascular abdominal aortic aneurysm repair: A word of caution. *J Vasc Surg.* 2008;47:886–892.
- Thomas B, Sanchez L. Proximal migration and endoleak: impact of endograft design and deployment techniques. *Semin Vasc Surg.* 2009;22:201–206.
- Rödel SGJ, Geelkerken RH, Prescott RJ, et al. The Anaconda AAA Stent Graft System: 2-year clinical and technical results of a multicentre clinical evaluation. *Eur J Vasc Endovasc Surg.* 2009;38:732–740.
- Freyrie A, Gallitto E, Gargiulo M, et al. Results of the endovascular abdominal aortic aneurysm repair using the Anaconda aortic endograft. *J Vasc Surg.* 2014;60:1132–1139.
- Saratzis N, Melas N, Saratzis A, et al. Anaconda aortic stent-graft: single-center experience of a new commercially available device for abdominal aortic aneurysms. *J Endovasc Ther.* 2008;15:33–41.
- Rödel SGJ, Zeebregts CJ, Huisman AB, et al. Results of the Anaconda endovascular graft in abdominal aortic aneurysm with a severe angulated infra-renal neck. *J Vasc Surg.* 2014;59:1495–1501.e1.
- Freyrie A, Gallitto E, Gargiulo M, et al. Proximal aortic neck angle does not affect early and late EVAR outcomes: an Anaconda™ Italian Registry analysis. *J Cardiovasc Surg (Torino).* 2014;55:671–677.
- Stella A, Freyrie A, Gargiulo M, et al. The advantages of Anaconda endograft for AAA. *J Cardiovasc Surg (Torino).* 2009;50:145–152.
- Freyrie A, Testi G, Faggioli GL, et al. Ring-stents supported infra-renal aortic endograft fits well in abdominal aortic aneurysms with tortuous anatomy. *J Cardiovasc Surg (Torino).* 2010;51:467–474.
- Ahn SS, Rutherford RB, Johnston KW, et al. Reporting standards for infra-renal endovascular abdominal aortic aneurysm repair. *J Vasc Surg.* 1997;25:405–410.
- Fitz-Henry J. The ASA classification and peri-operative risk. *Ann R Coll Surg Engl.* 2011;93:185–187.
- Harris PL, Buth J, Mialhe C, et al. The need for clinical trials of endovascular abdominal aortic aneurysm stent-graft repair: the EUROSTAR Project. *J Endovasc Ther.* 1997;4:72–77.
- Balm R, Stokking R, Kaatee R, et al. Computed tomographic angiographic imaging of abdominal aortic aneurysms: implications for transfemoral endovascular aneurysm management. *J Vasc Surg.* 1997;26:231–237.
- Bungay P. The use of the Anaconda™ stent graft for abdominal aortic aneurysms. *J Cardiovasc Surg (Torino).* 2012;53:571–577.
- Vascutek, a TERUMO company. Anaconda AAA Stent Graft System. Instructions for Use. [http://www.vascutek.com/site/assets/files/1586/301-130\\_2\\_anaconda\\_full\\_language\\_ifu-1.pdf](http://www.vascutek.com/site/assets/files/1586/301-130_2_anaconda_full_language_ifu-1.pdf). Accessed May 21, 2017.
- Klein A, Kroon D-J, Hoogeveen Y, et al. Multimodal image registration by edge attraction and regularization using a B-spline grid. *Proc SPIE.* 2011;7962:796220–796228.
- Klein A. A tool for studying the motion of stent grafts in AAA. In: *Segmentation and Motion Estimation of Stent Grafts in Abdominal Aortic Aneurysms* [dissertation]. Enschede, the Netherlands: University of Twente; 2011:121–137. doi:10.3990/1.9789036532662.
- Koenrades MA, Struijs EM, Klein A, et al. Validation of an image registration and segmentation method to measure stent graft motion on ECG-gated CT using a physical dynamic stent graft model. *Proc SPIE.* 2017;10134:1013411–1013418.
- Klein A, van der Vliet JA, Oostveen LJ, et al. Automatic segmentation of the wire frame of stent grafts from CT data. *Med Image Anal.* 2012;16:127–139.
- Stockel D. Nitinol—a material with unusual properties. *Endovasc Update.* 1998;(1):1–5.
- Cao P, Verzini F, Parlani G, et al. Predictive factors and clinical consequences of proximal aortic neck dilatation in 230 patients undergoing abdominal aorta aneurysm repair with self-expandable stent-grafts. *J Vasc Surg.* 2003;37:1200–1205.
- Dalainas I, Nano G, Bianchi P, et al. Aortic neck dilatation and endograft migration are correlated with self-expanding endografts. *J Endovasc Ther.* 2007;14:318–323.
- Dillavou ED, Muluk S, Makaroun MS. Is neck dilatation after endovascular aneurysm repair graft dependent? Results of 4 US Phase II trials. *Vasc Endovascular Surg.* 2005;39:47–54.
- Oberhuber A, Buecken M, Hoffmann M, et al. Comparison of aortic neck dilatation after open and endovascular repair of abdominal aortic aneurysm. *J Vasc Surg.* 2012;55:929–934.
- Monahan TS, Chuter TAM, Reilly LM, et al. Long-term follow-up of neck expansion after endovascular aortic aneurysm repair. *J Vasc Surg.* 2010;52:303–307.
- Soberón AB, de Garcia MM, Möll GG, et al. Follow-up of aneurysm neck diameter after endovascular repair of abdominal aortic aneurysms. *Ann Vasc Surg.* 2008;22:559–563.
- Sternbergh WC, Money SR, Greenberg RK, et al. Influence of endograft oversizing on device migration, endoleak, aneurysm shrinkage, and aortic neck dilation: Results from the Zenith multicenter trial. *J Vasc Surg.* 2004;39:20–26.

31. Filis KA, Galyfos G, Sigala F, et al. Proximal aortic neck progression: before and after abdominal aortic aneurysm treatment. *Front Surg*. 2017;4:1–6.
32. Malas MB, Ohki T, Veith FJ, et al. Absence of proximal neck dilatation and graft migration after endovascular aneurysm repair with balloon-expandable stent-based endografts. *J Vasc Surg*. 2005;42:639–644.
33. Peirano MAM, Bertoni HG, Chikiar DS, et al. Size of the proximal neck in AAAs treated with balloon-expandable stent-grafts: CTA findings in mid-to long-term follow-up. *J Endovasc Ther*. 2009;16:696–707.
34. Wolinsky H. Comparison of medial growth of human thoracic and abdominal aortas. *Circ Res*. 1970;27:531–538.
35. Zettervall SL, Soden PA, Deery SE, et al. Comparison of renal complications between endografts with suprarenal and infrarenal fixation. *Eur J Vasc Endovasc Surg*. 2017;54:5–11.